CHAPTER VII
PETROCHEMICAL AND FUELS PRODUCTION USING HBETA AND HIERARCHICAL MESOPOROUS MSU-S_{BEA} CATALYST IN BIO-ETHANOL DEHYDRATION AS A FUNCTION OF TIME-ON-STREAM

7.1 Abstract

Microporous HBeta and the hierarchical mesoporous MSU-S with Beta seed, denoted as MSU-S_{BEA} was synthesized by using tetraethylammonium hydroxide (TEAOH) as a structure directing agent and cetyltrimethylammonium bromide (CTAB) as a surfactant were employed as catalysts for the dehydration of bio-ethanol to studied the catalytic activity and product distributions at 450 °C for 24, 48, and 72 hours time-on-stream. The results from using HBeta exhibited that ethylene selectivity rapidly increased after 8 hours TOS due to the deactivation of strong acid sites, resulting in the decrement of p-xylenes and C_{10+} aromatics selectivity with increasing TOS. Meanwhile, MSU-S_{BEA} gave a high selectivity of ethylene in the gas stream and a high selectivity of non-aromatics in the oil, which was mostly composed of heavy olefins such as cetene and 7-hexadecene due to its milder acidity and large pore size. Moreover, the catalysts were characterized for their stability. It was found that although the structure was not destroyed during bio-ethanol dehydration, HBeta gave a poorer catalytic stability than MSU-S_{BEA} because it was fully deposited by coke with almost totally loss of its acidity after 1 day. Moreover, the partial dealumination at the surface of HBeta was observed after 3 days TOS. Furthermore, the structure of MSU-S_{BEA} was also not destroyed during bio-ethanol dehydration, but MSU-S_{BEA} provided a lower deactivation rate, indicated by the gradual decrease in acidity and a remaining high surface area and pore volume after 3 days.

7.2 Introduction

Petrochemical compounds such as BTEX are very high valuable products. One of the best known is p-xylene, which is the raw material for manufacturing

fibers and films, and the most important product is polyethylene terephthalate (PET). Non-aromatic compounds such as paraffins and olefins with a carbon number around 6 to 20 atoms are used as synthetic fuels, polymers, and detergents. Especially for synthetic fuel applications, the fuel quality was significantly affected by C10+ aromatics fraction since the fuel should contain a low amount of aromatic compounds (Haveling *et al.*, 1998).

Moreover, various types of zeolites had been investigated to produce hydrocarbons from dehydration of bio-ethanol. Takahara *et al.* (2005) studied ethanol to ethylene over solid catalysts using HZSM-5 with Si/Al ratio of 25 and 90, HBeta with Si/Al ratio of 25, HY with Si/Al ratio of 5.5, HMOR with Si/Al ratio of 20 and 90, and silica-alumina. The products of the dehydration of ethanol were ethylene, diethyl ether, ethane, propene, and butenes. Park and Seo (2009) studied methanol to olefins reaction over several zeolites using CHA, LTA, MFI, BEA, MOR, and FAU. They found that BEA, MFI, and FAU were selectively produce $C5^+$ and alkylaromatics. Although microporous zeolites can be used as the catalysts in bio-ethanol dehydration process, the huge problem of microporous zeolites is diffusion limitation. Large hydrocarbon molecules cannot pass throughout the pore, and causes coking that decreases the efficiency of the catalysts. So, to overcome this problem, hierarchical mesoporous materials have been synthesized and applied. Liu *et al.* (2001) developed the hierarchical mesoporous MSU-S (Michigan State University) with hexagonal structure synthesized from Beta (BEA) and ZSM-5 (MFI) seed using cetyltrimethylammonium bromide (CTAB) as a surfactant. The hierarchical mesoporous MSU-S, which is the composite of MCM-41 and zeolites seed, has been used in many applications. In 2013, Rashidi *et al.* studied methanol dehydration to dimethyl ether using MSU-S as a catalyst. They found that the activity and selectivity of MSU-S were higher than Al-MCM-41.

In addition, Sujeerakulkai and Jitkarnka (2014) studied bio-ethanol dehydration using the hierarchical mesoporous MSU-S with Beta-seed (MSU-S_{BEA}) as a catalyst. The result showed that the hierarchical mesoporous MSU-S_{BEA} exhibited high ethanol conversion at 97.4 %, ethylene was the main component (about 93 %) in the gas stream. Moreover, the large amount of xylenes, C_9, and C_{10+} aromatics were produced in the oil because of the large pore size of the catalyst,

which improved the diffusion limitation for large hydrocarbon molecules. Moreover, mesoporous catalysts also have been studied in ethylene oligomerization. Hulea and Fajula (2004) studied Ni exchanged Al-MCM-41 for ethylene oligomerization. The result exhibited that the large pore size of the catalyst can increase the diffusion of branch-chain oligomers, and the amount of oligomer increases with decreasing acid density. Furthermore, the higher acid density and high temperature were favorable oligomerized C_4 and C_6 olefins into C_{8+} hydrocarbons.

Generally, the stability of the hierarchical mesoporous catalysts is higher than microporous catalysts due to their large pore size which the large hydrocarbon molecules can pass throughout the pore and that can reduce coking. From the literatures review, the large pore size of catalysts should be employed in order to produce fuel range products. In this work, microporous HBeta zeolite and hierarchical mesoporous MSU-S_{BEA} were studied in comparison for bio-ethanol dehydration in order to investigate the product distribution and catalytic activity that may alter with different time-on-streams. The catalysts were tested for 24 to 72 hours time-on-stream, respectively. Subsequently, they were characterized for investigating their stability.

7.3 Experimental

7.3.1 Catalyst Preparation

7.3.1.1 Synthesis of MSU-S_{BEA}

To prepare the BEA-seed solution, a mixture of Al-(i-BuO)$_3$ (0.02 mol) and TEOS (0.98 mol) were added to a stirred solution of aqueous TEAOH (35 wt%, 0.37 mol) in H_2O (20 mol). After aging for about 2 hours, the solution was transferred into a Teflon-line autoclave, and hydrothermally treated at 100 °C for 3 hours to form BEA-seeds. After that, the seed solution was added to a solution of CTAB (0.25 mol) in H_2O (127 mol). The solution was adjusted to a pH of 9.0 by using sulfuric acid (0.17 mol). The resulting synthesis gel was then hydrothermally treated in a Teflon-lined autoclave at 150 °C for 2 days to form the mesostructure. The solution was next filterd, washed, dried, and calcined at 2 °C/min to 550 °C for 4

hours to obtain the MSU-S_{BEA} catalysts. (Liu *et al.*, 2001; Triantafyllidis *et al.*, 2007).

7.3.1.2 Commercial Zeolites

HBeta zeolite (BEA, NH_4-form, SiO_2/Al_2O_3 = 37 mol/mol, BET surface area = 502 m^2/g, Zeolyst International, USA) was used in this work. HBeta was calcined at 550 °C, 2 °C/min for 6 hours to obtain the H-form and remove impurities. Then, the calcined catalyst was hydraulically pressed to pellets. Next, the pellets were crushed and sieved to 20 - 40 mesh particles before use in the reactor. The abbreviations of catalysts used in the experiments are shown in Table 7.1.

7.3.2 Catalyst Characterization

The surface area (BET), pore volume (Horvath Kawazoe method), and pore size (Barret-Joyner-Halenda method) were determined based on N_2 physisorption using the Thermo Finnigan/Sorptomatic 1990. Rigaku TTRAX III was used in the small-angle mode to determine the Small Angle X-Ray Scattering (SAXS) pattern of MSU-S_{BEA} from 1°-7° with the scan speed of 1 °/min. For the wide-angled, Rigaku Smartlab® was used to determine from 5°-50° with the scan speed of 5°/min with the increment of 0.01. The bulk and surface Si/Al_2 ratio of the synthesized MSU-S_{ZSM-5} was determined by X-ray Fluorescence spectrometry (XRF) and X-ray Photoelectron Spectroscopy (XPS), respectively. X-ray fluorescence spectrometry (AXIOS PW4400) was used to determine the bulk Si/Al ratio of the fresh and spent catalysts. The conditions were set as follows: internal flow of 4.10 l/min, external flow of 2.49 l/min, cabinet temperature of 29.97 °C, primary temperature of 19.00 °C, vacuum of 10.10 Pa, x-ray generation of 50 kV (60 mA), 150 μm of collimator, angle of 10.0002 degree, gas flow 0.90 l/h, and gas pressure of 1020.8 hPa. XPS was used to determine the Si/Al ratio on the surface of the fresh and spent catalysts. The scan pass energy was 160 kV for wide scan and 40 kV for narrow scan. The electron source was Al Kα that gave 10 mA of emission and 15 kV of anode HT. The neutralizer was set at 1.8 A of filament current, 2.6 V of charge balance, and 1.3 V of filament bias. Temperature Programmed Desorption (TPD-NH_3) was also used to determine the acidity of the catalysts. Acid properties such as

acid strength and acidity were determined by Thermo Finnigan 1100. 0.2 g of a catalyst was treated by nitrogen flow at 300 °C for 3 hours. Then, after the catalyst was cooled down to room temperature, it was added with 10 % v/v NH_3 of helium balance with a flow of 20 ml/min. The NH_3-TPD profiles were obtained by heating the reactor at 10 °C/min up to 800 °C with helium flow of 20 ml/min. After that, the desorbed gases were analyzed by TCD detector. Transmission Electron Microscopy (TEM) was used to determine the hexagonal structure of MSU-S_{ZSM-5}. The mixture of a catalyst powder and ethanol was sonicated for 20 min. After that, the mixture was dropped onto copper grid with a Formvar support, and then dried. Hitachi H-7501 SS in TEM high-resolution (HR) mode took images using a voltage of 100 kV. In addition, the coke formation on catalysts was determined by a Thermogravimetric/Differential Thermal Analyzer (TG/DTA). The spent catalysts were weighed and placed in a Pt pan followed by heating from 50 to 900 °C with the heating rate of 10 °C /min. Nitrogen and oxygen flow rate were controlled at 100 ml/min and 200 ml/min, respectively.

Table 7.1 Nomenclature of catalysts used in the experiments

# of run	Catalyst	Abbreviation
1	HBeta at 1 day time-on-stream	HB-S1
2	HBeta at 2 days time-on-stream	HB-S2
3	HBeta at 3 days time-on-stream	HB-S3
4	MSU-S_{BEA} at 1 day time-on-stream	MSU-B-S1
5	MSU-S_{BEA} at 2 days time-on-stream	MSU-B-S2
6	MSU-S_{BEA} at 3 days time-on-stream	MSU-B-S3

7.3.3 Bio-ethanol Dehydration

The purified bio-ethanol (99.5 % purity) was obtained from Sapthip Co., Ltd., Thailand. The catalytic dehydration of bio-ethanol was conducted in a U-tube fixed bed reactor (10 mm, inside diameter and 45.8 cm, length) with 3 grams of catalyst under atmospheric pressure at 450 °C by collecting data at every 4 hours for 24, 48, and 72 hours. Bio-ethanol was fed at 2 ml/hour co-fed with helium at 13.725 ml/min. The gas compositions were analyzed by using a GC-TCD (Agilent 6890N),

and a GC-FID (Agilent 6890N) was used to determine the ethanol concentration. Ice bath was employed to condense the oil from the gas stream. Then, the oil product was extracted from the liquid product by using CS_2. Then, a Simdist GC was used to determine the true boiling point curve of oil. The range of boiling points indicates the type of petroleum products; <149.°C for gasoline, 149-232 °C for kerosene, 232-343 °C for gas oil, 343-371 °C for light vacuum gas oil, and >371 °C for high vacuum gas oil (Dũng *et al.*, 2009). In addition, the oil composition was determined by using Gas Chromatograph equipped with a Mass Spectrometry of "Time of Flight" type (GC - GC- TOF/MS) (installed with Rxi-5SilMS and RXi-17 consecutive columns). The conditions were set as follows: the initial temperature of 50°C held for 30 minutes, the heating rate of 2 °C/min from 50 to 120 °C, and 10 °C/min from 120 to 310 °C with split ratio of 5.

7.4 Results and Discussion

7.4.1 Characterization of HBeta and MSU-S_{BEA}

Rikagu TTRAX was used to determine the Small Angle X-ray Scattering patterns (SAXS) of MSU-S_{BEA} in the range of 1-7° and Rikagu Smartlab® was employed to determine XRD spectra of the catalyst in the wide angle-mode (5-50°). Figure 7.1 illustrates the XRD patterns of MSU-S_{BEA} compared to that of HBeta, which can be seen that MSU-S_{BEA} provides a sharp peak around 2.2° and a broad peak around 22°, which indicate that MSU-S_{BEA} with a hexagonal structure and a semi-crystalline structure was successfully synthesized. The result from XRF shows that HBeta and MSU-S_{BEA} have the Si/Al_2 ratio of 33.5 and 75.6, respectively.

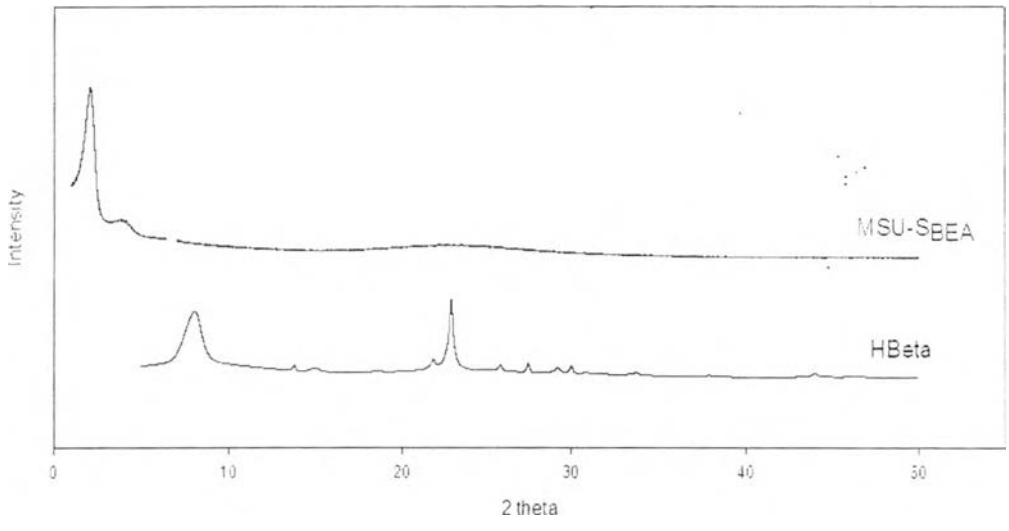

Figure 7.1 XRD patterns of MSU-S_{BEA} and HBeta.

Moreover, Figure 7.2(a) shows the N_2 adsorption-desorption isotherm of MSU-S_{BEA}, which illustrates the sudden step at P/P_0 around 0.35, and (b) also shows pore size distribution of MSU-S_{BEA}. Table 7.2 illustrates the surface area, pore volume, micropore and mesopore diameters of HBeta and MSU-S_{BEA} calculated by Horvath Kawazoe and Barret-Joyner-Halenda method, respectively. MSU-S_{BEA} exhibits the higher surface area and pore volume than that of HBeta. The micropore and mesopore diameters of MSU-S_{BEA} are 7.56 Å and 26.77 Å, respectively. Additionally, the TPD-NH_3 profiles of HBeta and MSU-S_{BEA} are shown in Figure 7.3. It can be noted that both HBeta and MSU-S_{BEA} have 2 peaks which indicate that they have 2 types of acid sites. HBeta contains the weak acid sites around 80 %, which the NH_3 desorption peak is present at 150 °C, and has 20.% stronger acid sites present at 460 °C. In contrast, the TPD-NH_3 profile of MSU-S_{BEA} indicates the stronger acid site is dominant and present at 551 °C, which account for about 58 %. It can be stated that the stronger acid sites might be the acid sites from the beta seed, and the weaker might be the acid sites from MSU-S. Additionally, both weak and strong acid sites of MSU-S_{BEA} are stronger than those of HBeta.

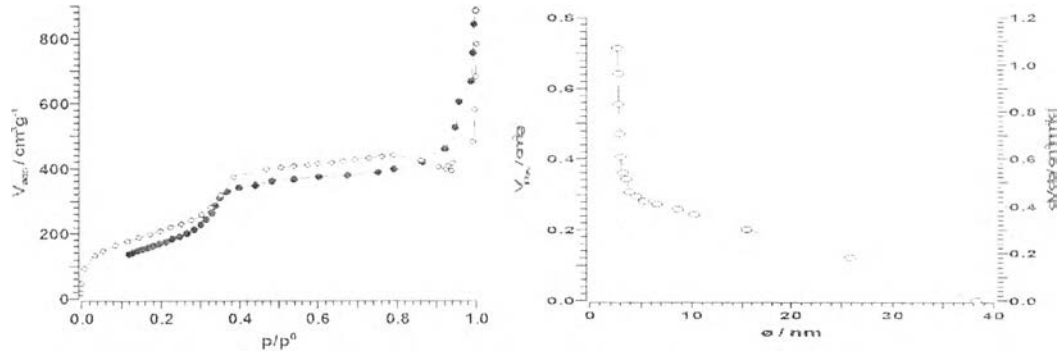

Figure 7.2 (a) N_2 adsorption-desorption isotherm, and (b) pore size distribution of MSU-S_{BEA} using B.J.H. method.

Table 7.2 Physical properties of HBeta and MSU-S_{BEA}

Catalysts	Si/Al_2 Ratio	Surface Area (m^2/g) [a]	Pore Volume (cm^3/g) [b]	Micropore Diameter (Å)[b]	Mesopore Diameter (Å)[c]
HBeta	33.5	502.0	0.26	7.93	-
MSU-S_{BEA}	75.6	821.2	0.43	7.56	26.77

[a] Determined by BET method, [b] Determined by H.K. method, and [c] Determined by B.J.H. method

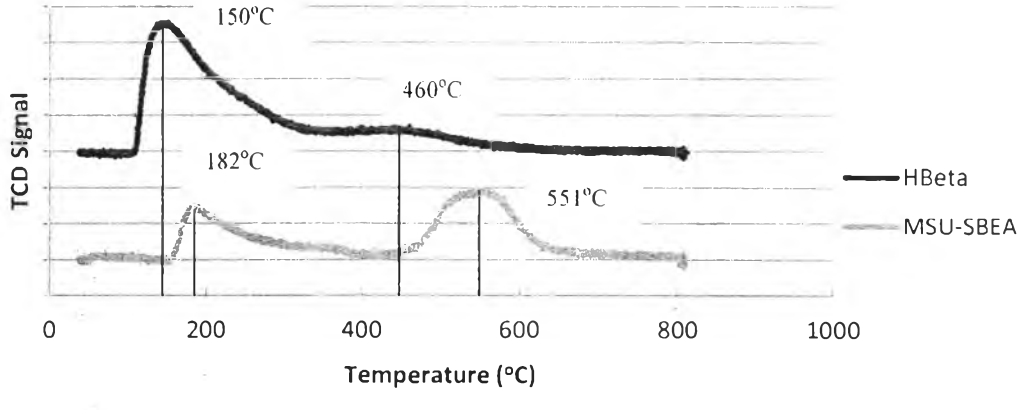

Figure 7.3 TPD-NH_3 profiles of HBeta and MSU-S_{BEA}.

7.4.2 Stability of HBeta and MSU-S_{BEA}

After the reaction, the spent HBeta and MSU-S_{BEA} at various TOSs were characterized to determine their textural properties by using XRD and Surface Area Analyzer. Figure 7.4(a) illustrates the XRD patterns of HBeta, which can be seen that the intensity of the characteristic peak at 8.10° decreases after 1 day time-on-stream. However, the intensity of characteristic peak at 22.82° increases with increasing TOS. The corresponding d_{302} spacing decreasing from 3.893 Å to 3.886 Å is observed after 3 days TOS, indicating that there is some removal of Al atoms from the zeolite framework (Baran *et al.*, 2012). Furthermore, the SAXS patterns of spent MSU-S_{BEA} show a lower intensity and a little shift to more angles with increasing TOS as shown in Figure 7.4(b), indicating that it has smaller pore size and poorer pore structure alignment (Thanabodeekij *et al.*, 2006). Moreover, X-ray Photoelectron Spectroscopy (XPS) and X-ray Fluorescence (XRF) were used to determine the surface and bulk Si/Al_2 ratio of HBeta and MSU-S_{BEA}. The results from XRF indicate that the bulk Si/Al_2 ratios of both HBeta and MSU-S_{BEA} gives no significant changes. However, the Si/Al_2 ratio at the surface of HB-S3 increases almost 30 % from the fresh one, indicating that HBeta is partially dealuminated at the surface after 3 days of TOS as shown in Figure 7.5(a). Gonzalez *et al.* (2011) stated that HBeta was easy to dealuminate due to the flexibility of its framework, pore arrangement, and size. In addition, the variations of surface vs bulk Si/Al_2 values of MSU-S_{BEA} are present near the diagonal line, indicating that the hexagonal structure of MSU-S is a thin wall, which is composed of each beta seed and Al atom likely present at the outer surface of the wall as shown in Figure 7.5(b).

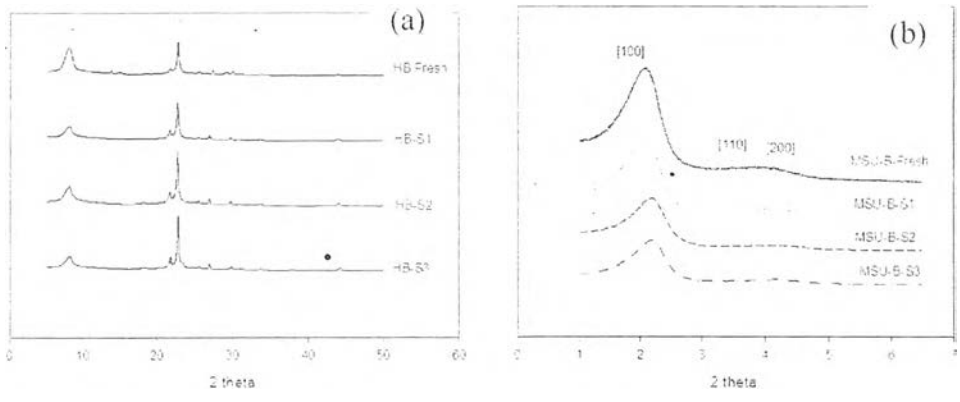

Figure 7.4 XRD patterns of HBeta (a) and (b) SAXS patterns of MSU-S_{BEA}.

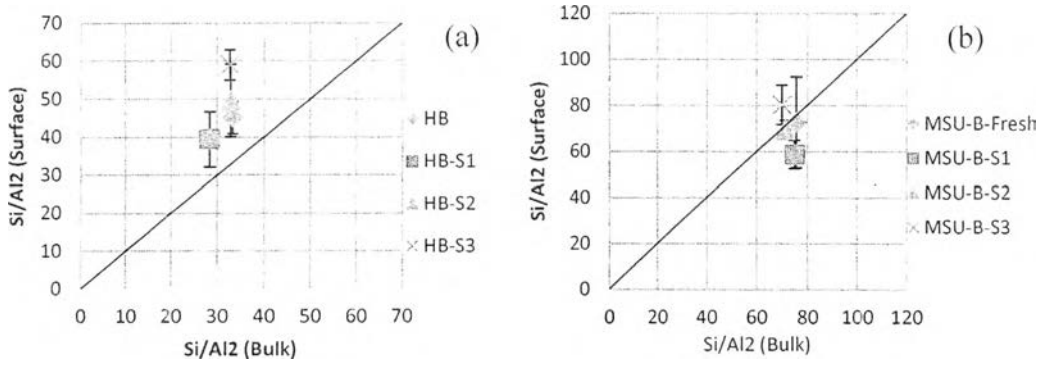

Figure 7.5 Variation of surface Si/Al_2 vs. bulk Si/Al_2 ratios of (a) HBeta and (b) MSU-S_{BEA} (Moreno and Poncelet, 1997).

Although the XRD patterns show that structure of HBeta is not destroyed during 3 days of bio-ethanol dehydration, coke is fully deposited after 1 day whereas MSU-S_{BEA} keeps its high surface area after 3 days due to its large pore size, which can improve the diffusion of large hydrocarbons as shown in Figure 7.6(a) and (b) and Figure 7.7 exhibits the coking rate of HBeta and MSU-S_{BEA} that HBeta has much higher coking rate than MSU-S_{BEA}. It can be seen that coking rate of both catalysts decrease with increasing TOS which means coke molecules deposit on the acid sites and prevent the transformation of ethylene to higher hydrocarbons. Furthermore, Figure 7.8 illustrates the TPD-NH_3 profiles from using (a) HBeta and (b) MSU-S_{BEA}. Both HBeta and MSU-S_{BEA} exhibit two peaks, which represent the different acid

types on the catalysts, and it can be seen that MSU-S_{BEA} exhibits the higher temperature for both peaks, which means both weak and strong acid of MSU-S_{BEA} are stronger than those of HBeta. Moreover, HBeta has high density of weak acid site about 80 % at 150 °C and 20 % stronger acid site at 460 °C. Moreover, the strong acid type present at 551°C is dominant (59 %) in the TPD-NH_3 profile of MSU-S_{BEA} whereas the rest is weaker acid sites present at 182 °C. After 1 day TOS, the acidity of HBeta rapidly decreases, indicated by a disappearance of a strong acid peak and a great decrease of a weak acid peak, and then the weak acid peak gradually decreases with increasing TOS. The explanation might be the coke is almost fully deposited in HBeta after 1 day TOS. In addition, the strong acid site of MSU-S_{BEA} is the first to be lost by the reaction and coke deposition, which can be seen by the shift to the lower temperature of the strong acid peak, and then the decrease of weak acid peak, respectively.

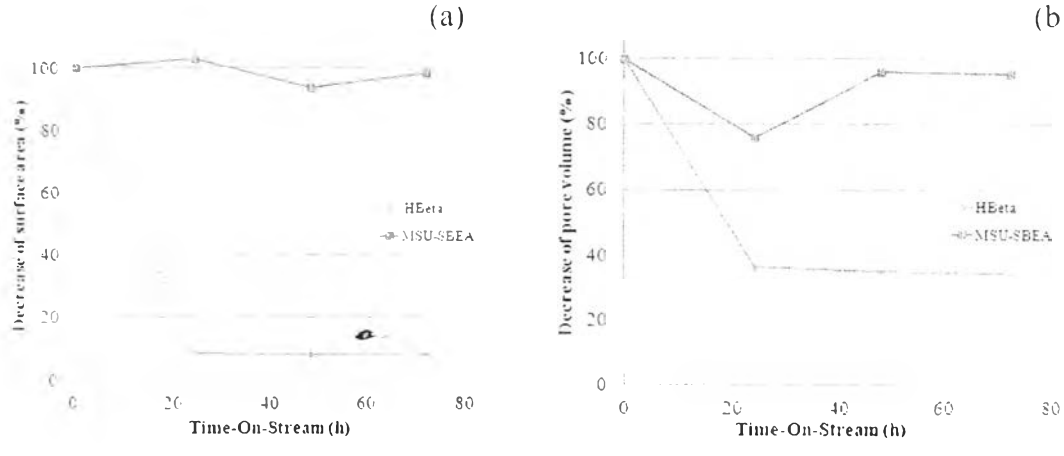

Figure 7.6 Decreases of surface area and pore volume of (a) HBeta, and (b) MSU-S_{BEA}

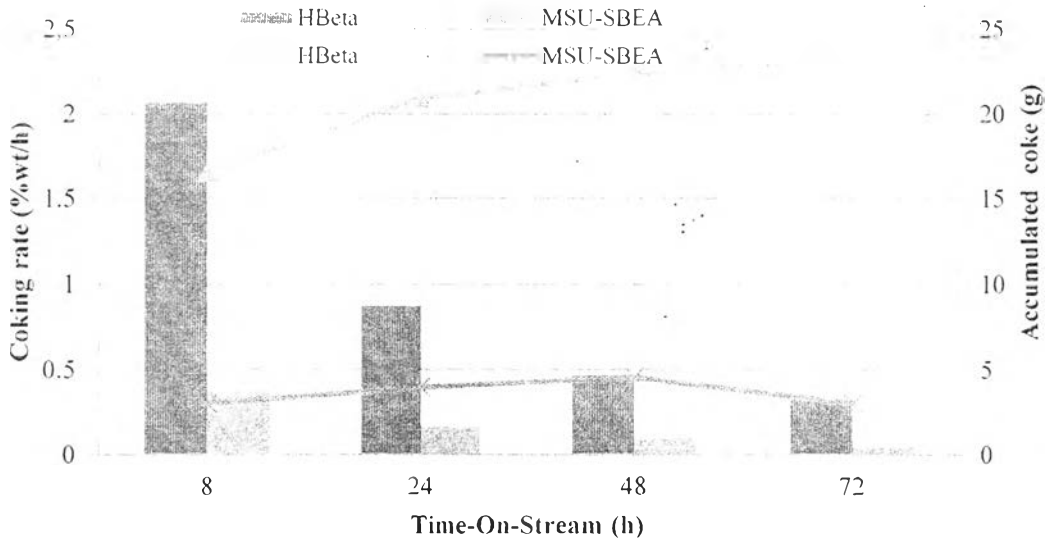

Figure 7.7 Coking rates and accumulated coke of HBeta and MSU-S_{BEA}.

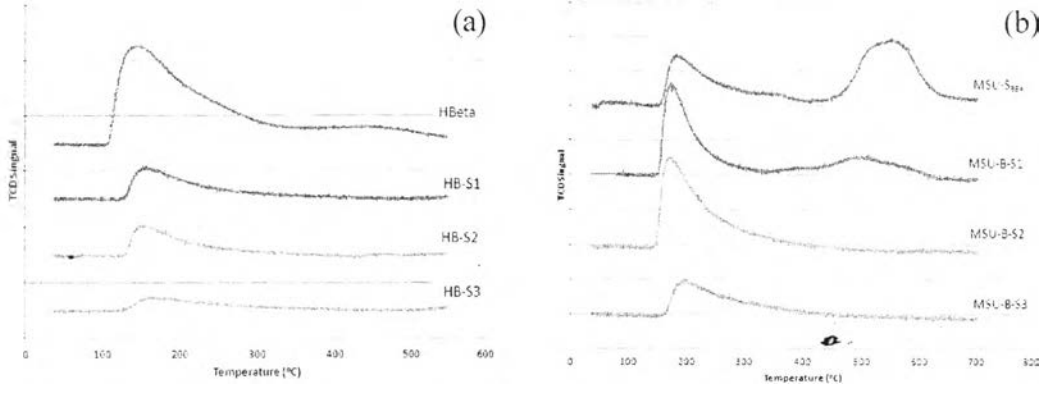

Figure 7.8 TPD-NH_3 profiles of (a) HBeta and (b) MSU-S_{BEA} at various TOSs.

7.4.3 Comparison of HBeta and MSU-S_{BEA} as Catalysts

7.4.3.1 Conversion and Gas Product

The concentration profiles of gaseous products and bio-ethanol conversion from using HBeta are shown in Figure 7.9(a) and (b). Ethylene selectivity rapidly increases during the first 8 hours of time-on-stream in the opposite way with propane and mixed C_4 selectivity. After 60 hours of time-on-stream, ethylene becomes the only component in the gas stream. However, about 99 % bio-ethanol conversion is achieved along TOS. Furthermore, MSU-S_{BEA} exhibits a high

selectivity of ethylene in the concentration profiles of gaseous products, and provides as high as about 100 % bio-ethanol conversion along TOS as shown in Figure 7.9(c) and (d).

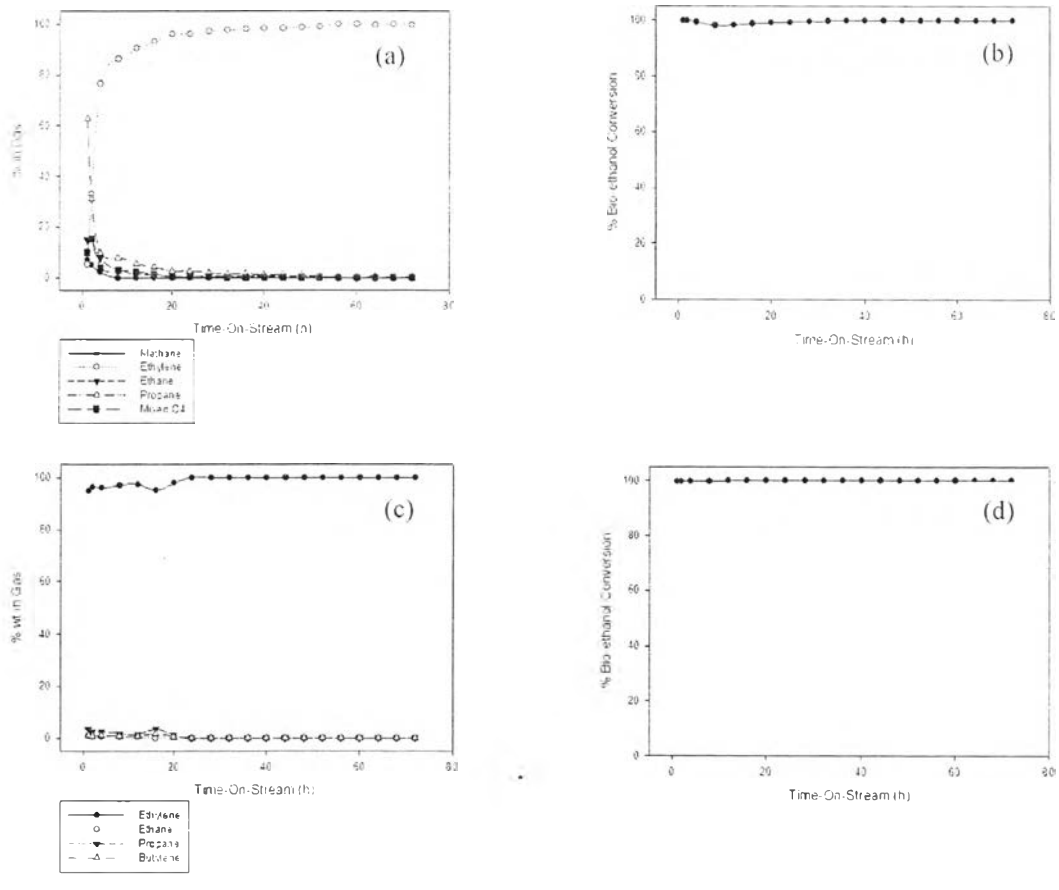

Figure 7.9 (a) Concentration profiles of gas components and (b) bio-ethanol conversion using HBeta as a catalyst, (c) concentration profiles of gas components and (d) bio-ethanol conversion using MSU-S_{BEA}.

7.4.3.2 Petroleum Fractions of Oil

Moreover, Figure 7.10(a) shows the petroleum fractions of the obtained oil from HBeta at various TOSs. Kerosene is the majority in the oil, followed by gasoline and gas oil, accordingly because the large pore size and strong acidity of HBeta are proper for the production of large hydrocarbons. However, the increasing time-on-stream affects to the decrease of gas oil. Furthermore, the results from TGA indicate that the amount of coke deposition in HBeta increases with

increasing TOS. It can be stated that polyaromatic hydrocarbons can be condensed, and then block the porous system of HBeta, which the adsorption and reaction of ethylene cannot occur, resulting in the decrease of heavier oil fraction (Madeira *et al.*, 2009; Pinard *et al.*, 2013). In contrast, the results from MSU-S_{BEA} shows that the increases of gas oil and light vacuum gas oil fractions with increasing TOS are observed as shown in Figure 7.10(b) due to its large pore size and milder acidity that are proper for the formation of large hydrocarbon molecules. Moreover, the results from TGA exhibit that MSU-S_{BEA} gives a lower amount of coke deposition (about 4 %wt) due to its large pore size that can enhance the diffusion of large hydrocarbons.

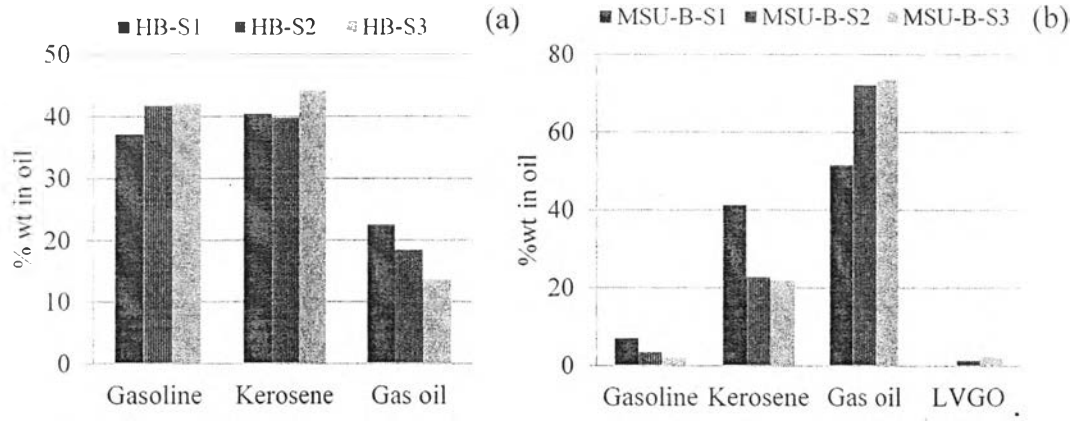

Figure 7.10 (a) Petroleum fractions of HBeta, and (b) MSU-S_{BEA} at various TOSs.

7.4.3.3 Oil Composition

The oil compositions of HBeta at different TOSs are shown in Figure 7.11(a). After 1 day TOS, the obtained oil from HBeta is mostly composed of p-xylene, C_9, and C_{10+} aromatics due to the large pore size and high acidity of HBeta, which are suitable for the production of large hydrocarbons. However, when TOS increases, p-xylene and C_{10+} aromatics selectivity decrease in the opposite way with benzene, toluene, and C_9 aromatics. Moreover, it can be referred to the results of TGA from Figure 7.7 that the accumulated coke deposition increases with increasing TOS. It can be noted that the suppression of p-xylene and C_{10+} aromatics selectivity are caused by the coke formation in HBeta, and these cokes are trapped in

the pore of HBeta, which can be deposited on the acid sites and then block the pore. Thus, further reactions could not be occurred, then resulting in the decreased selectivity of large hydrocarbons (Madeira *et al.*, 2009).

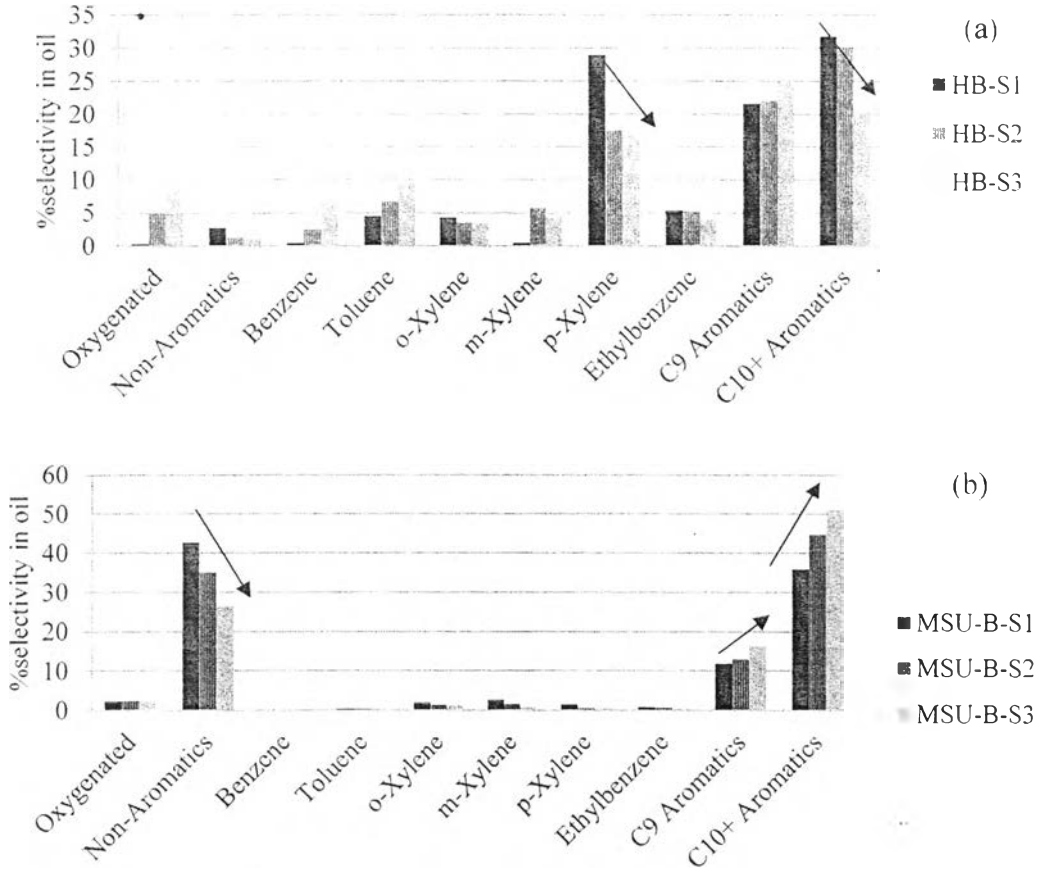

Figure 7.11 Oil compositions obtained from (a) HBeta and (b) MSU-S_{BEA} with various TOSs.

Based on the oil compositions obtained from MSU-S_{BEA} in Figure 7.11(b), the main groups of components are non-aromatics, C_9, and C_{10+} aromatics. As time-on-stream increases, non-aromatic fraction and mixed xylenes tend to decrease adversely with C_9 and C_{10+} aromatics due to dehydrocyclization of olefins to form aromatic compounds (Ramasamy and Wang, 2013). Table 7.3 exhibits the content of hydrocarbons in non-aromatic fraction, which indicates that the straight chain hydrocarbons become more cyclic hydrocarbons with increasing

TOS. In addition, the main group of components in non-aromatic fraction is olefins. Furthermore, Figure 7.12 shows the carbon number distribution in non-aromatic fraction. It is clearly seen that C_{16} is the main fraction in non-aromatics, and most of C_{16} olefins are 7-hexadecene and cetene that can be indicated as diesel components (Haveling *et al.*, 1998) whereas 1-pentene is the main specie in C_6, and 1,3,5-cycloheptatriene, 7-ethyl is the main specie in C_9. The large pore size and mild acidity of MSU-S_{BEA} can promote the oligomerization and dimerization of olefins into non-aromatic products with a low selectivity of aromatic hydrocarbons.

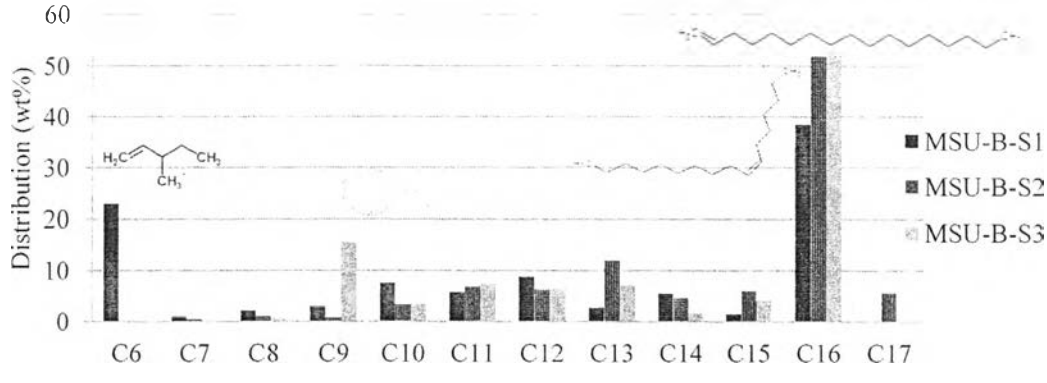

Figure 7.12 Carbon number distributions in non-aromatic fraction obtained from MSU-S_{BEA} at various TOSs.

Table 7.3 Hydrocarbons in non-aromatic fraction based on structure

Catalyst	Straight Chain (%wt)	Cyclic (%wt)
MSU-B-S1	95.25	4.75
MSU-B-S2	93.72	6.28
MSU-B-S3	80.66	19.34

7.4.4 Reaction Pathways of HBeta and MSU-S_{BEA}

According to the results from the previous section, it has been shown that bio-ethanol conversion of HBeta and MSU-S_{BEA} was almost 100 % during 72 hours TOS. The concentration profiles of gaseous products from HBeta showed that

ethylene selectivity drastically increased at the begining due to the fast deactivation of strong acid sites whereas MSU-S_{BEA} with a large pore size gave a high ethylene selectivity along TOS. Moreover, the fast deactivation of HBeta can suppress the potential to transform ethylene into higher hydrocarbons, resulting in the lower selectivity of p-xylene and C_{10+} aromatics with increasing TOS. Furthermore, due to the micropore structure and strong acid sites of HBeta, aromatic hydrocarbons can undergo alkylation, hydrogen transfer, Sullivan mechanism, and rearrangement reaction, forming polyaromatics depositing on the acid sites and then blocking the pore (Pinard *et al.*, 2013), so it prevents the transformation of ethylene into higher hydrocarbons.

On the other hand, the oil of MSU-S_{BEA} highly contained of non-aromatic fraction due to its milder acidity and larger pore size, compared to that of HBeta. At initial, oligomerization of ethylene can be occurred at the micropore of Beta-seeds, forming C_4-C_6 olefins, and then these olefins can further oligomerize or dimerize in the mesopore of MSU-S_{BEA}, forming larger oligomeric molecules such as C_8-C_{16} compounds as shown in Figure 7.13. Moreover, based on the pathways discussed in Hulea and Fajula (2004) the reaction pathways of ethylene oligomerization in the pore of MSU-S_{BEA} can be explained as follows. Firstly, two molecules of ethylene can be oligomerized, forming C_4 olefins in the micropore of Beta seed. Subsequently, double bond isomerization of C_4 - C_8 olefins occurs at weak acid sites at a high temperature. Furthermore, C_4 – C_6 olefins can undergo dimerization in the mesopore of MSU-S_{BEA}, forming the higher molecular-weight olefins such as C_8 or C_{12}, which favored by strong acid sites and C_{16} olefins might be undergo dimerization from C_8 olefins.

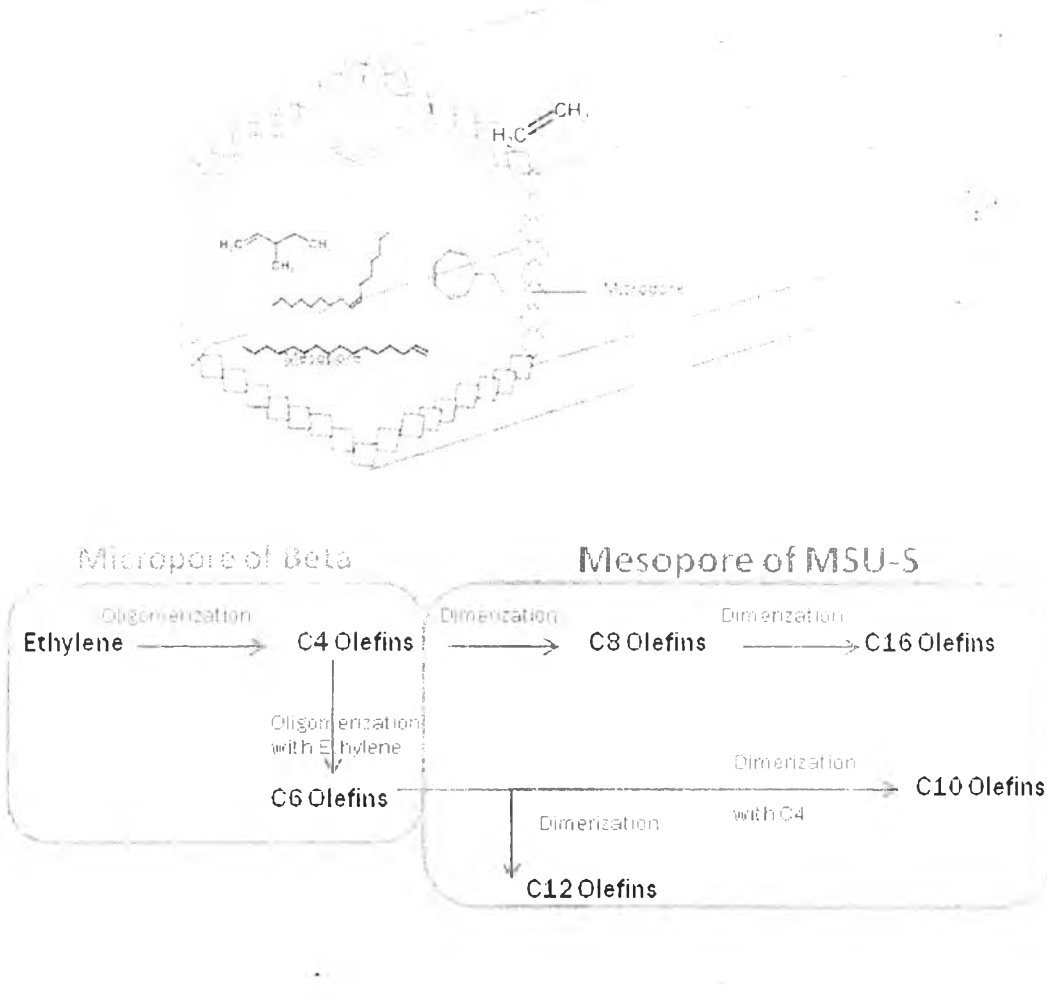

Figure 7.13 Possible reactions in the micro-mesopore of MSU-S_{BEA}.

7.5 Conclusions

A microporous HBeta with Si/Al_2 ratio of 37, and the synthesized hierarchical mesoporous MSU-S_{BEA} with Si/Al_2 ratio of 75.6 were used in the catalytic dehydration of bio-ethanol with various TOSs. HBeta showed the fast deactivation, resulting in the increment of ethylene selectivity in the gas stream and the decrement of p-xylene and C_{10+} aromatics selectivity in the oil composition due to polyaromatics condensation in the pore of HBeta, which prevented the reactions of ethylene by coking on the acid sites and pore blocking. In contrast, for MSU-S_{BEA}, the heavy petroleum fractions such as gas oil and light vacuum gas oil tended to increase with increasing TOS due to its large pore size that can enhance the diffusion

of hydrocarbons. Moreover, the oil from MSU-S_{BEA} mostly consisted of non-aromatics, C_9, and C_{10+} aromatics fractions. The non-aromatic fraction, which was mostly composed of olefins, tended to transform into C_9 and C_{10+} aromatics via aromatization reaction. According to the spent catalysts characterization, it can be stated that MSU-S_{BEA} had better catalytic activity and stability than that of HBeta. Although the XRD patterns indicated that the structure of both catalysts still maintained after 3 days of bio-ethanol dehydration, coke was fully deposited on HBeta after 1 day, and the dealumination occurred after 3 days whereas MSU-S_{BEA} still had high surface area after 3 days TOS.

7.6 Acknowledgements

This work was carried out with the financial support of Center of Excellent on Petrochemical and Materials Technology (PETROMAT), Chulalongkorn University, and Sapthip Co., Ltd for bio-ethanol.

7.7 References

Baran, R., Millot, Y., Onfroy, T., Krafft, J.M., and Dzwigaj, K. (2012) Influence of the nitric acid treatment on Al removal, framework composition and acidity of BEA zeolite investigated by XRD, FTIR and NMR. Microporous and Mesoporous Materials, 163, 122-130.

Dũng, N.A., Kaewkla, R., Wongkasemjit, S., and Jitkarnka, S. (2009) Light olefins and light oil production from catalytic pyrolysis of waste tire. Journal of Analytical and Applied Pyrolysis, 86, 281-286.

González, M.D., Cesteros, Y., and Salagre, P. (2011) Comparison of dealumination of zeolites beta, mordenite and ZSM-5 by treatment with acid under microwave irradiation. Microporous and Mesoporous Materials, 144, 162-170.

Haveling, J., Nicolaides, C.P., and Scurrell, M.S. (1998) Catalysts and conditions for the highly efficient, selective and stable heterogeneous oligomerisation of ethylene. Applied Catalysis A, 173(10), 1-9.

Hulea, V. and Fajula, F. (2004) Ni-exchanged AlMCM-41—An efficient bifunctional catalyst for ethylene oligomerization. Journal of Catalysis, 225(1), 213-222.

Liu, Y., Zhang, W., and Pinnavaia, T.J. (2001) Steam-stable aluminosilicate mesostructures assembled from zeolite ZSM-5 and zeolite Beta-seeds. J. Am. Chem. Soc., 122, 8791-8792.

Lourenço, J.P., Fernandes, A., Henriques, C, and Ribeiro, M.F. (2006) Al-containing MCM-41 type materials prepared by different synthesis methods: Hydrothermal stability and catalytic properties. Microporous and Mesoporous Materials, 94(1-3), 56-65.

Madeira, F.F., Gnep, N.S., Magnoux, P., Maury, S., and Cadran, N. (2009) Ethanol transformation over HFAU, HBEA and HMFI zeolites presenting similar Brønsted acidity. Applied Catalysis A, 367(1-2), 39-46.

Moreno, S. and Poncelet, G. (1997) Dealumination of small- and large-port mordenites: a comparative study. Microporous Materials, 12, 197-222.

Park, D.H., Kim, S.S., Pinnavaia, T.J., Tzompanzi, F., Prince, J., and Valente, J.S. (2011) Selective isobutene oligomerization by mesoporous MSU-S_{BEA} catalysts. Journal of Physical Chemistry, 115(13), 5809-5816.

Park, J.W. and Seo, G. (2009) IR study on methanol-to-olefin reaction over zeolites with different pore structures and acidities. Applied Catalysis A, 356(2), 180-188.

Pinard, L., Hamieh, S., Canaff, C., Madeira, F.F., Batonneau-Gener, I., Maury, S., Delpoux, O., Ben Tayeb, K., Pouilloux, Y., and Vezin, H. (2013) Growth mechanism of coke on HBEA zeolite during ethanol transformation. Journal of Catalysis, 299, 284-297.

Ramasamy, K.K., Zhang, H., Sun, J., and Wang Y. (2014) Conversion of ethanol to hydrocarbons on hierarchical HZSM-5 zeolites. Catalysis Today, 238, 103-110.

Ramasamy, K.K. and Wang, Y. (2013) Catalyst activity comparison of alcohols over zeolites. Journal of Energy Chemistry, 22, 65-71.

Rashidi, H., Hamoule, T., Nikou, M.R.K., and Shariati, A. (2013) DME synthesis over MSU-S catalyst through methanol dehydration reaction. Iranian Journal of Oil & Gas Science and Technology, 2 (4), 67-73.

Sujeerakulkai, S. and Jitkarnka, S. (2014) Bio-ethanol dehydration to hydrocarbons using Ga_2O_3/Beta zeolites with various Si/Al_2 ratios. Chemical Engineering Transactions, 39, 967-972

Takahara, I., Saito, M., Inaba, M., and Murata, K. (2005) Dehydration of ethanol into ethylene over solid acid catalysts. Catalysis Letters, 105(3-4), 249-252.

Thanabodeekij, N., Sadthayanon, S., Gulari, E., and Wongkasemjit, S. (2006) Extremely high surface area of ordered mesoporous MCM-41 by atrane route. Materials Chemistry and Physics, 98, 131-137.

Triantafyllidis, K.S., Iliopoulou, E.F., Antonakou, E.V., Lappas, A.A., Wang, H., and Pinnavaia, T.J. (2007) Hydrothermally stable mesoporous aluminosilicates (MSU-S) assembled from zeolite seeds as catalysts for biomass pyrolysis. Microporous and Mesoporous Materials, 99(1-2), 132–139.